# Renormalized relativistic Hartree-Bogoliubov equations with a zero-range pairing interaction

T. Nikšić and P. Ring

*Physik-Department der Technischen Universität München, D-85748 Garching, Germany*

D. Vretenar

*Physics Department, Faculty of Science,*

*University of Zagreb, Zagreb, Croatia*

(Dated: February 9, 2008)



## Abstract

A recently introduced scheme for the renormalization of the Hartree-Fock-Bogoliubov equations in the case of zero-range pairing interaction is extended to the relativistic Hartree-Bogoliubov model. A density-dependent strength parameter of the zero-range pairing is adjusted in such a way that the renormalization procedure reproduces the empirical $^1S_0$ pairing gap in isospin-symmetric nuclear matter. The model is applied to the calculation of ground-state pairing properties of finite spherical nuclei.

PACS numbers: 21.30.Fe, 21.60.Jz, 21.65.+f, 21.10.-k

## I. INTRODUCTION

The theoretical framework of self-consistent mean-field models enables a description of the nuclear many-body problem in terms of universal energy density functionals. By employing global effective interactions, adjusted to empirical properties of symmetric and asymmetric nuclear matter, and to bulk properties of spherical nuclei, the current generation of self-consistent mean-field models has achieved a high level of accuracy in the description of ground states and properties of excited states in arbitrarily heavy nuclei, exotic nuclei far from $\beta$-stability, and in nuclear systems at the nucleon drip-lines [1].

The relativistic mean-field (RMF) models, in particular, are based on concepts of non-renormalizable effective relativistic field theories and density functional theory. They have been very successfully applied in studies of nuclear structure phenomena at and far from the valley of $\beta$-stability. For a quantitative analysis of open-shell nuclei it is necessary to consider also pairing correlations. Pairing has often been taken into account in a very phenomenological way in the BCS model with the monopole pairing force, adjusted to the experimental odd-even mass differences. This approach, however, presents only a poor approximation for nuclei far from stability. The physics of weakly-bound nuclei necessitates a unified and self-consistent treatment of mean-field and pairing correlations. This has led to the formulation and development of the relativistic Hartree-Bogoliubov (RHB) model, which represents a relativistic extension of the conventional Hartree-Fock-Bogoliubov framework, and provides a basis for a consistent microscopic description of ground-state properties of medium-heavy and heavy nuclei, low-energy excited states, small-amplitude vibrations, and reliable extrapolations toward the drip lines [2].

In most applications of the RHB model [2] the pairing part of the well known and very successful Gogny force [3] has be employed in the particle-particle ($pp$) channel:

$$V^{pp}(1,2) \;=\; \sum_{i=1,2} e^{-((\mathbf{r}_1-\mathbf{r}_2)/\mu_i)^2} \left(W_i \;+\; B_i P^\sigma - H_i P^\tau - M_i P^\sigma P^\tau\right) , \tag{1}$$

with the set D1S [4] for the parameters $\mu_i$, $W_i$, $B_i$, $H_i$, and $M_i$ ($i = 1, 2$). This force has been very carefully adjusted to the pairing properties of finite nuclei all over the periodic table. In particular, the basic advantage of the Gogny force is the finite range, which automatically guarantees a proper cut-off in momentum space. However, the resulting pairing field is non-local and the solution of the corresponding Dirac-Hartree-Bogoliubov integro-differential

equations can be time-consuming, especially in the case of deformed nuclei. Another possibility is the use of a zero-range, possibly density-dependent, $\delta$-force in the $pp$-channel of the RHB model [5]. This choice, however, introduces an additional cut-off parameter in energy and neither this parameter, nor the strength of the interaction, can be determined in a unique way. The effective range of the interaction is determined by the energy cut-off, and the strength parameter must be chosen accordingly in order to reproduce empirical pairing gaps.

In a series of recent papers [6, 7, 8] A. Bulgac and Y. Yu have introduced a simple scheme for the renormalization of the Hartree-Fock-Bogoliubov equations in the case of zero-range pairing interaction. The scheme is equivalent to a simple energy cut-off with a position dependent coupling constant. In this work we use the prescription of Refs. [6, 7] to implement a regularization scheme for the relativistic Hartree-Bogoliubov equations with zero-range pairing. We analyze the resulting $^1S_0$ pairing gap in isospin-symmetric nuclear matter and apply the RHB model to the calculation of ground-state pairing properties of finite spherical nuclei.

In Sec. II we present an outline of the RHB model and introduce the renormalization scheme for the case of zero-range pairing. The model is applied in Sec. III to pairing in isospin-symmetric nuclear matter. Ground-state pairing properties of Sn nuclei are analyzed in Sec. IV. Sec. V contains the summary and conclusions.

## II. RELATIVISTIC HARTREE-BOGOLIUBOV MODEL WITH ZERO-RANGE PAIRING

A detailed review of the relativistic Hartree-Bogoliubov model can be found, for instance, in Ref. [2]. In this section we include those features which are essential for the discussion of the renormalization of the RHB equations. The model can be derived within the framework of covariant density functional theory. When pairing correlations are included, the energy functional depends not only on the density matrix $\hat{\rho}$ and the meson fields $\phi_m$, but in addition also on the anomalous density $\hat{\kappa}$

$$E_{RHB}[\hat{\rho},\hat{\kappa},\phi_m] = E_{RMF}[\hat{\rho},\phi_m] + E_{pair}[\hat{\kappa}] \ , \tag{2}$$

where $E_{RMF}[\hat{\rho},\phi]$ is the RMF energy density functional and the pairing energy $E_{pair}[\hat{\kappa}]$ is given by

$$E_{pair}[\hat{\kappa}] = \frac{1}{4}\mathrm{Tr}\left[\hat{\kappa}^* V^{pp}\hat{\kappa}\right]. \tag{3}$$

$V^{pp}$ denotes a general two-body pairing interaction. The equation of motion for the generalized density matrix

$$\mathcal{R} = \begin{pmatrix} \rho & \kappa \\ -\kappa^* & 1-\rho^* \end{pmatrix}, \tag{4}$$

reads

$$i\partial_t \mathcal{R} = [\mathcal{H}(\mathcal{R}), \mathcal{R}] \ . \tag{5}$$

The generalized Hamiltonian $\mathcal{H}$ is a functional derivative of the energy with respect to the generalized density

$$\mathcal{H}_{RHB} \ = \ \frac{\delta E_{RHB}}{\delta \mathcal{R}} \ = \ \begin{pmatrix} \hat{h}_D - m - \mu & \hat{\Delta} \\ -\hat{\Delta}^* & -\hat{h}_D^* + m + \mu \end{pmatrix}. \tag{6}$$

The self-consistent mean field $\hat{h}_D$ is the Dirac Hamiltonian, and the pairing field reads

$$\Delta_{ab}(\mathbf{r},\mathbf{r}') = \frac{1}{2}\sum_{c,d} V^{pp}_{abcd}(\mathbf{r},\mathbf{r}')\kappa_{cd}(\mathbf{r},\mathbf{r}'), \tag{7}$$

where $a, b, c, d$ denote quantum numbers that specify the Dirac indices of the spinors, and $V^{pp}_{abcd}(\mathbf{r},\mathbf{r}')$ are the matrix elements of a general two-body pairing interaction.

Pairing effects in nuclei are restricted to an energy window of a few MeV around the Fermi level, and their scale is well separated from the scale of binding energies, which are in the range of several hundred to thousand MeV. There is no experimental evidence for any relativistic effect in the nuclear pairing field $\hat{\Delta}$. Therefore, pairing can be treated as a non-relativistic phenomenon, and a hybrid RHB model with a non-relativistic pairing interaction can be employed. For a general two-body interaction, the matrix elements of the relativistic pairing field read

$$\hat{\Delta}_{a_1p_1,a_2p_2} = \frac{1}{2}\sum_{a_3p_3,a_4p_4} \langle a_1p_1, a_2p_2|V^{pp}|a_3p_3, a_4p_4\rangle_a \ \kappa_{a_3p_3,a_4p_4} \ , \tag{8}$$

where the indices $(p_1, p_2, p_3, p_4 = +, -)$ refer to the large and small components of the quasi-particle Dirac spinors. In most applications of the RHB model, only the large components

of the spinors $U_k(\mathbf{r})$ and $V_k(\mathbf{r})$ have been included in the non-relativistic pairing tensor $\hat{\kappa}$ in Eq. (12). The resulting pairing field reads

$$\hat{\Delta}_{a_1+,a_2+} = \frac{1}{2} \sum_{a_3+,a_4+} \langle a_1+, a_2+ | V^{pp} | a_3+, a_4+ \rangle_a \ \kappa_{a_3+,a_4+} \ . \tag{9}$$

The other components: $\hat{\Delta}_{+-}$, $\hat{\Delta}_{-+}$, and $\hat{\Delta}_{--}$ are neglected, in accordance with the results that are obtained with a relativistic zero-range force [10].

The ground state of an open-shell nucleus is described by the solution of the relativistic Hartree-Bogoliubov equations

$$\begin{pmatrix} \hat{h}_D - m - \mu & \hat{\Delta} \\ -\hat{\Delta}^* & -\hat{h}_D^* + m + \mu \end{pmatrix} \begin{pmatrix} U_k(\mathbf{r}) \\ V_k(\mathbf{r}) \end{pmatrix} = E_k \begin{pmatrix} U_k(\mathbf{r}) \\ V_k(\mathbf{r}) \end{pmatrix} \ , \tag{10}$$

which correspond to the stationary limit of Eq. (5).

The chemical potential $\mu$ is determined by the particle number subsidiary condition in order that the expectation value of the particle number operator in the ground state equals the number of nucleons. The column vectors denote the quasiparticle wave functions, and $E_k$ are the quasiparticle energies. The RHB wave functions determine the hermitian single-particle density matrix

$$\hat{\rho}_{ll'} = (V^* V^T)_{ll'}, \tag{11}$$

and the antisymmetric anomalous density

$$\hat{\kappa}_{ll'} = (V^* U^T)_{ll'}. \tag{12}$$

The calculated nuclear ground-state properties sensitively depend on the choice of the effective Lagrangian and pairing interaction. Over the years many parameter sets of the mean-field Lagrangian have been derived that provide a satisfactory description of nuclear properties along the $\beta$-stability line. The most successful RMF effective interactions are purely phenomenological, with parameters adjusted to reproduce the nuclear matter equation of state and a set of global properties of spherical closed-shell nuclei. This framework has recently been extended to include effective Lagrangians with explicit density-dependent meson-nucleon couplings. In a number of studies it has been shown that this class of global effective interactions provides an improved description of asymmetric nuclear matter, neutron matter and finite nuclei far from stability. In the present analysis of ground-state

properties of Sn isotopes the density-dependent effective interaction DD-ME1 [9] will be employed in the particle-hole ($ph$) channel of the RHB model.

In the following we extend the regularization scheme of Bulgac and Yu [6, 7, 8] to the solution of the relativistic Hartree-Bogoliubov equations for a zero-range pairing interaction

$$V^{pp}(\mathbf{r},\mathbf{r}') = g\delta(\mathbf{r}-\mathbf{r}') \ . \tag{13}$$

In Refs. [6, 7] it has been shown that in this case the renormalized pairing field can be expressed as

$$\Delta(\mathbf{r}) = -g_{\mathit{eff}}(\mathbf{r})\kappa_c(\mathbf{r}) \ , \tag{14}$$

where $\kappa_c(\mathbf{r})$ denotes the cut-off anomalous density

$$\kappa_c(\mathbf{r}) = \sum_{E_k>0}^{E_c} V_k^{\dagger}(\mathbf{r})U_k(\mathbf{r}) \ . \tag{15}$$

The cut-off energy $E_c$ defines the two corresponding momenta $k_c$ and $l_c$

$$\sqrt{k_c^2(\mathbf{r})+m^{*2}(\mathbf{r})} + V(\mathbf{r}) - m \ = \ E_c + \mu, \tag{16}$$

$$\sqrt{l_c^2(\mathbf{r})+m^{*2}(\mathbf{r})} + V(\mathbf{r}) - m \ = \ -E_c + \mu \ . \tag{17}$$

$m^*(\mathbf{r}) = m+S(\mathbf{r})$ is the Dirac mass, and $S(\mathbf{r})$ and $V(\mathbf{r})$ are, respectively, the scalar and vector single-nucleon potentials contained in the Dirac Hamiltonian $\hat{h}_D$. The chemical potential $\mu$ determines the local Fermi momentum

$$\sqrt{k_f^2(\mathbf{r})+m^{*2}(\mathbf{r})} + V(\mathbf{r}) - m = \mu \ . \tag{18}$$

The effective, position-dependent coupling in Eq. (14) reads

$$\frac{1}{g_{\mathit{eff}}(\mathbf{r})} = \frac{1}{g} + F_1(\mathbf{r}) + F_2(\mathbf{r}) \ , \tag{19}$$

with

$$\begin{aligned} F_1(\mathbf{r}) \ = \ & -\frac{k_c(\mathbf{r})\sqrt{k_f^2(\mathbf{r})+m^{*2}(\mathbf{r})}}{4\pi^2}\left[1-\frac{k_f(\mathbf{r})}{k_c(\mathbf{r})}\ \mathrm{Ar\ cth}\frac{k_c(\mathbf{r})}{k_f(\mathbf{r})}\right] \\ & -\frac{k_c(\mathbf{r})\sqrt{k_c^2(\mathbf{r})+m^{*2}(\mathbf{r})}}{8\pi^2} + \frac{\sqrt{k_f^2(\mathbf{r})+m^{*2}(\mathbf{r})}}{4\pi^2}\ k_f(\mathbf{r})\ \mathrm{Ar\ cth}\frac{k_c(\mathbf{r})\sqrt{k_f^2(\mathbf{r})+m^{*2}(\mathbf{r})}}{k_f(\mathbf{r})\sqrt{k_c^2(\mathbf{r})+m^{*2}(\mathbf{r})}} \\ & -\frac{2k_f^2(\mathbf{r})+m^{*2}(\mathbf{r})}{8\pi^2}\ \ln\frac{k_c(\mathbf{r})+\sqrt{k_c^2(\mathbf{r})+m^{*2}(\mathbf{r})}}{m^*(\mathbf{r})} \end{aligned} \tag{20}$$

$$
\begin{aligned}
F_2(\mathbf{r}) \;=\; & -\frac{l_c(\mathbf{r})\sqrt{k_f^2(\mathbf{r})+m^{*2}(\mathbf{r})}}{4\pi^2}\left[1-\frac{k_f(\mathbf{r})}{l_c(\mathbf{r})}\;\mathrm{Ar\;th}\frac{l_c(\mathbf{r})}{k_f(\mathbf{r})}\right] \\
& -\frac{l_c(\mathbf{r})\sqrt{l_c^2(\mathbf{r})+m^{*2}(\mathbf{r})}}{8\pi^2}+\frac{\sqrt{k_f^2(\mathbf{r})+m^{*2}(\mathbf{r})}}{4\pi^2}\;k_f(\mathbf{r})\;\mathrm{Ar\;th}\frac{l_c(\mathbf{r})\sqrt{k_f^2(\mathbf{r})+m^{*2}(\mathbf{r})}}{k_f(\mathbf{r})\sqrt{l_c^2(\mathbf{r})+m^{*2}(\mathbf{r})}} \\
& -\frac{2k_f^2(\mathbf{r})+m^{*2}(\mathbf{r})}{8\pi^2}\;\ln\frac{l_c(\mathbf{r})+\sqrt{l_c^2(\mathbf{r})+m^{*2}(\mathbf{r})}}{m^*(\mathbf{r})}
\end{aligned}
\tag{21}
$$

$F_1 + F_2$ is the relativistic generalization of the corresponding correction to the coupling constant $g$, as defined in Eq. (16) of Ref. [6].

## III. PAIRING PROPERTIES OF SYMMETRIC NUCLEAR MATTER

A zero-range pairing interaction leads to a particularly simple expression for the gap equation in symmetric nuclear matter

$$
\frac{1}{g_{\mathit{eff}}} = -\frac{1}{4\pi^2}\int_{l_c}^{k_c} dk\;\frac{k^2}{\sqrt{\left[\sqrt{k^2+m^{*2}}-\sqrt{k_f^2+m^{*2}}\;\right]^2+\Delta^2}}\;, \tag{22}
$$

The momenta $k_c$ and $l_c$ are determined by the cut-off energy $E_c$ Eqs. (16, 17), and the effective coupling $g_{\mathit{eff}}$ is defined in Eq. (19). In the left panel of Fig. 1 we display the density dependence of the resulting pairing gap in nuclear matter (dashed curve). The single-particle spectrum has been calculated with the relativistic effective interaction DD-ME1 [9], and the coupling constant of the zero-range pairing interaction Eq. (13) $g = -330$ MeV fm$^3$ is typical for the values used by Bulgac and Yu in their analyses. The pairing gap is shown in comparison to the gap calculated with the effective Gogny interaction D1S [4] (dots). The corresponding single-particle spectrum has been computed in the Hartree-Fock approximation for the Gogny interaction. The density dependence of the two gaps is completely different. The pairing gap of the renormalized zero-range interaction increases uniformly with density, whereas the gap of the Gogny interaction display the characteristic maximum of $\approx 2.5$ MeV at low density $\rho = 0.03 - 0.04$ fm$^{-3}$ (corresponding to a Fermi momentum of approximately 0.8 fm$^{-1}$) and decreases at higher densities. The bell-shaped form of the pairing gap as a function of the density was, in fact, obtained already more than forty years ago [12]. This density dependence is not characteristic only of the phenomenological finite-range interactions, but is also obtained when the gap is calculated with bare nucleon-nucleon potentials adjusted to the empirical nucleon-nucleon phase shifts and

deuteron properties (for a recent review see Ref. [13]). The decrease of the gap at Fermi momenta $k_f > 0.8$ fm$^{-1}$ simply reflects the repulsive character of the nucleon-nucleon interaction at short distances [11]. Of course there is no repulsive component in the zero-range force with constant coupling Eq. (13), and the corresponding pairing gap displays the unphysical uniform increase with density. We notice, however, that in the range of densities shown in Fig. 1, i.e. up to nuclear matter saturation density, the values of the pairing gap of the renormalized zero-range interaction are comparable with those of the Gogny pairing gap. As will be shown in the next section, this means that the renormalization scheme for the zero-range interaction with constant coupling can be safely applied to the calculation of pairing correlations in finite nuclei, provided an appropriate choice is made for the strength parameter $g$.

On the other hand, there is no particular reason why the strength parameter $g$ of the zero-range pairing interaction should be a constant. In fact, in many applications to finite nuclei an explicit density dependence is introduced, and in this way pairing correlations partially include finite-range effects. For instance, in one of the first applications [14] Bertsch and Esbensen used a density-dependent contact interaction, together with a simple energy cut-off, in a description of pairing correlations in weakly bound neutron-rich nuclei. They also compared the corresponding pairing gap in symmetric nuclear matter with the result of a Hartree-Fock calculation using the Gogny interaction. In the present anaysis we have adjusted a density-dependent strength parameter $g(\rho)$ of the zero-range pairing interaction Eq. (13), in such a way that the pairing gap of the renormalized zero-range interaction Eq. (22), reproduces the density dependence of the Gogny pairing gap. The resulting density dependence can be approximated by the following analytic expression

$$g(\rho) = \frac{1}{a_0 + a_1\rho^{1/3} + a_2\rho^{2/3}} \ , \tag{23}$$

with $a_0 = -0.064$ fm$^{-2}$, $a_1 = 0.447$ fm$^{-1}$, and $a_2 = -3.693$. The resulting pairing gap, displayed in the left panel of Fig. 1 (solid line), is in very good agreement with the one calculated using the Gogny interaction. A very similar procedure was employed in Ref.[15], where the density dependence of the "bare coupling constant" $g(\rho)$ was adjusted to a specific formula for the pairing gap in low-density homogeneous neutron matter.

In the right panel of Fig. 1 we display the effective couplings $g_{\mathit{eff}}$ calculated using the constant $g = -330$ MeV fm$^3$, and the density dependent coupling of Eq. (23). The density

dependence of the two effective couplings is completely different. In order to prevent an unphysical growth of the pairing gap with density, the density dependence of the pairing strength Eq. (23) ensures that the effective coupling becomes weaker with increasing nucleon density. A very strong effective coupling in the low-density region produces a peak in the corresponding pairing gap shown in the left panel. On the other hand, $g_{\mathit{eff}}$ calculated using the constant coupling increases in absolute value with density, i.e. the resulting pairing gap increases uniformly with density. However, rather similar values for the two effective couplings $g_{\mathit{eff}}$ are calculated in the region of densities characteristic for the bulk of finite nuclei. One should not, therefore, expect very different results for the pairing properties of finite nuclei calculated with the zero-range interaction with constant coupling, or with the density-dependent coupling of Eq. (23). In the next section we will show that this is really not true in weakly-bound nuclei far from stability.

The renormalization prescription must, of course, lead to a pairing field which is independent of the cut-off energy $E_c$, if the latter is chosen large enough. This is illustrated in Fig. 2, where we plot the pairing gap, calculated using the density-dependent coupling of Eq. (23), for a number of characteristic values $E_c$ in the interval between 5 MeV and 60 MeV. The pairing gap shows a weak dependence on the cut-off energy only for the two lowest values of $E_c$. When the cut-off is increased beyond 10 MeV, the corresponding pairing gaps cannot be distinguished. Thus already for $E_c \geq 10$ MeV the pairing gap of the renormalized zero-range interaction in symmetric nuclear matter converges. This is in agreement with the results obtained in the analysis of the pairing gap in homogeneous neutron matter [6].

## IV. GROUND-STATE PAIRING PROPERTIES OF SPHERICAL NUCLEI

In this section the renormalization scheme is tested in the calculation of ground-state pairing properties of Sn isotopes. The DD-ME1 mean-field Lagrangian is employed for the *ph* channel, and the zero-range interaction Eq. (13) is used in the *pp* channel. The renormalization procedure described in the previous section is carried out for the zero-range interaction with constant pairing strength $g = -330$ MeV fm$^3$, and and for the density-dependent coupling of Eq. (23). In the latter case the density dependence of the pairing strength has been adjusted to reproduce the Gogny D1S pairing gap in symmetric nuclear matter. In the following we denote by RCC the case of the renormalized constant coupling,

and by RDDC the results obtained with the renormalized density-dependent coupling.

While in the symmetric nuclear matter the Fermi momentum is always real (see Eq. (18)), in the surface region of finite nuclei it becomes imaginary. In Ref. [6] it has been shown that also in this case the renormalized anomalous density is real. The effective coupling $g_{\mathit{eff}}$ is still given by Eq. (19), but

$$
\begin{aligned}
F_1(\mathbf{r}) \;=\; & -\frac{k_c(\mathbf{r})\sqrt{-|k_f(\mathbf{r})|^2+m^{*2}(\mathbf{r})}}{4\pi^2}\left[1-\frac{k_f(\mathbf{r})}{k_c(\mathbf{r})}\ \mathrm{Ar\ ctg}\frac{k_c(\mathbf{r})}{k_f(\mathbf{r})}\right] \\
& -\frac{k_c(\mathbf{r})\sqrt{k_c^2(\mathbf{r})+m^{*2}(\mathbf{r})}}{8\pi^2}+\frac{\sqrt{-|k_f(\mathbf{r})|^2+m^{*2}(\mathbf{r})}}{4\pi^2}\ k_f(\mathbf{r})\ \mathrm{Ar\ ctg}\frac{k_c(\mathbf{r})\sqrt{-|k_f(\mathbf{r})|^2+m^{*2}(\mathbf{r})}}{k_f(\mathbf{r})\sqrt{k_c^2(\mathbf{r})+m^{*2}(\mathbf{r})}} \\
& -\frac{(-2|k_f(\mathbf{r})|^2+m^{*2}(\mathbf{r}))}{8\pi^2}\ \ln\frac{k_c(\mathbf{r})+\sqrt{k_c^2(\mathbf{r})+m^{*2}(\mathbf{r})}}{m^*(\mathbf{r})}\ , \qquad (24)
\end{aligned}
$$

and

$$
F_2(\mathbf{r})=0\ . \qquad (25)
$$

However, if either $k_c$ or $l_c$ becomes imaginary, the corresponding terms in the effective coupling should be omitted.

The rate of convergence of the renormalization scheme is illustrated in Fig. 3 where, for the nucleus $^{114}$Sn, we display the average pairing gaps and the pairing energies as functions of the cut-off energy $E_c$. The average gaps shown in the left panel, are defined as

$$
<\Delta_N>=\frac{\sum_{nlj}\Delta_{nlj}v^2_{nlj}}{\sum_{nlj}v^2_{nlj}}\ , \qquad (26)
$$

where $v^2_{nlj}$ are the occupation probabilities of the neutron states in the canonical basis. Both the pairing gaps and the pairing energies converge already for $E_c \geq 10$ MeV. We also notice that, even though the renormalized constant coupling and the renormalized density-dependent coupling lead to very different pairing gaps in symmetric nuclear matter, in $^{114}$Sn they produce similar average pairing gaps and virtually identical pairing energies.

The corresponding pairing fields as functions of the radial coordinate, and $g_{\mathit{eff}}$ Eq. (19) as functions of the density, are plotted in Fig. 4 for a series of values of the energy cut-off. In both cases the calculation of the pairing field and $g_{\mathit{eff}}$ shows convergence for $E_c > 10$ MeV. While the renormalized constant coupling and the renormalized density-dependent coupling produce very similar average pairing gaps and pairing energies, the dependence of the corresponding pairing fields on the radial coordinate is rather different. The RCC

pairing field (upper left panel) is concentrated in the bulk of the nucleus, whereas the RDDC pairing field (lower left panel) exhibits a pronounced peak on the surface. This behavior reflects the difference between the effective couplings $g_{\mathit{eff}}$, already shown in the right panel of Fig. 1 for the case of symmetric nuclear matter. In the panels on the right of Fig. 4 we plot the effective couplings $g_{\mathit{eff}}(r(\rho))$ as functions of the nucleon density in $^{114}$Sn. The $g_{\mathit{eff}}$ which corresponds to the density-dependent coupling of Eq. (23) decreases steeply in the region of very low density, i.e., on the surface of the nucleus. Consequently, also the pairing field displays a peak in the surface region. In both the RCC and RDDC cases the pronounced discontinuity of the effective coupling $g_{\mathit{eff}}$ at very low density corresponds to the transition from real to imaginary Fermi momentum $k_f$. This is illustrated in Fig. 5, where we plot the effective single-nucleon potential (left panel) and the correction to the coupling originating from the renormalization of the anomalous density (right panel). The effective single-nucleon potential is determined by the sum of the vector and scalar potentials $V_{cen}(\mathbf{r}) = S(\mathbf{r}) + V(\mathbf{r})$. For real values of the Fermi momentum (the effective potential is below the chemical potential $\mu$) the correction to the coupling $F_1(\mathbf{r}) + F_2(\mathbf{r})$ is calculated from Eqs. (20) and (21), and for imaginary values of the Fermi momentum (the effective potential is above the chemical potential $\mu$) from Eqs. (24) and (25). In the region where the Fermi momentum changes from real to imaginary the correction $F_1(\mathbf{r}) + F_2(\mathbf{r})$ displays a very sharp peak, which is reflected in the discontinuities of the effective couplings.

The importance of possible surface effects is illustrated in Fig. 6, where we plot the calculated average pairing gaps and pairing energies for the chain of even-even Sn isotopes with $110 \leq A \leq 160$. Although both the RCC and RDCC schemes lead to comparable values of the average pairing gaps for the entire isotopic chain, the pairing energies differ significantly for isotopes beyond the doubly closed-shell $^{132}$Sn. For example, the pairing energy of $^{150}$Sn calculated with renormalized density-dependent coupling (RDDC) is almost 25 MeV larger than the one calculated with the renormalized constant coupling (RCC). The large increase in the pairing energy for the RDDC case is caused by the dominant role of the surface region for the very neutron-rich Sn isotopes, and because the effective coupling is especially strong at very low densities. In the panels on the left of Figs. 7 and 8 we plot the self-consistent solutions for the cut-off anomalous densities Eq. (15) for the isotopes $^{114}$Sn, $^{124}$Sn and $^{150}$Sn, calculated using the RDDC and RCC effective couplings, respectively. The corresponding effective couplings $g_{\mathit{eff}}$ are shown in the panels on the right of Figs. 7 and 8.

The anomalous densities for $^{114}$Sn and $^{124}$Sn are concentrated in the nuclear volume ($r \leq 6$ fm), where the effective couplings $g_{eff}$ have comparable values. Therefore, the corresponding pairing energies are similar for the RDDC and RCC cases. In $^{150}$Sn, on the other hand, the anomalous densities extend to the region $r \geq 8$ fm, where the RDDC effective coupling becomes much stronger than the one calculated with the constant coupling (RCC). Hence, the pairing energy for $^{150}$Sn, calculated using the renormalized density-dependent coupling is much larger than the one obtained with the renormalized constant coupling.

## V. CONCLUSIONS

A simple renormalization scheme for the Hartree-Fock-Bogoliubov equations with zero-range pairing has recently been introduced [6, 7, 8]. In the present work we have implemented this renormalization scheme for the relativistic Hartree-Bogoliubov equations with a zero-range pairing interaction. The procedure is equivalent to a simple energy cut-off with a position dependent coupling constant. We have verified that the resulting average pairing gaps and pairing energies do not depend on the cut-off energy $E_c$, if the latter is chosen large enough. Convergence is achieved already for values $E_c \geq 10$ MeV, both in nuclear matter and for finite nuclei. If the strength parameter of the zero-range pairing is a constant, the resulting pairing gap in symmetric nuclear matter displays an unphysical increase with density. We have therefore adjusted a density-dependent strength parameter of the zero-range pairing in such a way that the renormalization procedure reproduces in symmetric nuclear matter the pairing gap of the phenomenological Gogny interaction. In this sense the present study goes beyond the simple extension of the renormalization scheme of Ref. [6] to the relativistic framework. However, the resulting effective coupling is too strong in the region of low density, and this leads to large pairing energies in open-shell nuclei with very diffuse surfaces, e.g. in neutron-rich Sn isotopes. One must therefore be careful when applying the renormalized HFB or RHB models with zero-range pairing to nuclei far from stability. Adjusting the strength parameter to the pairing gap in symmetric nuclear matter obviously does not provide enough information about the density dependence of the zero-range pairing to be used in very neutron-rich nuclei.

## ACKNOWLEDGMENTS

This work has been supported in part by the Bundesministerium für Bildung und

Forschung - project 06 MT 193, by the Alexander von Humboldt Stiftung, and by the Croatian Ministry of Science - project 0119250.

---

[1] M. Bender, P.-H. Heenen, and P.-G. Reinhard, Rev. Mod. Phys. 75 (2003) 121.

[2] D. Vretenar, A.V. Afanasjev, G.A. Lalazissis, and P. Ring, Phys. Rep. (2005).

[3] J.F. Berger, M. Girod, and D. Gogny, Nucl. Phys. A 428, 23c (1984).

[4] J. F. Berger, M. Girod, and D. Gogny, Commput. Phys. Commun. 63, 365 (1991).

[5] J. Meng, Nucl. Phys. A 635, 3 (1998).

[6] A. Bulgac, Phys. Rev. C 65, 051305 (2002).

[7] A. Bulgac and Y. Yu, Phys. Rev. Lett. 88, 042504 (2002).

[8] Y. Yu and A. Bulgac, Phys. Rev. Lett. 90, 222501 (2003).

[9] T. Nikšić, D. Vretenar, P. Finelli, and P. Ring, Phys. Rev. C 66, 024306 (2002).

[10] M. Serra and P. Ring, Phys. Rev. **C65**, 064324 (2002).

[11] M. Serra, A. Rummel, and P. Ring, Phys. Rev. **C65**, 014304 (2002).

[12] V.J. Emery and A.M. Sessler, Phys. Rev. **119**, 248 (1960).

[13] D.J. Dean and M. Hjorth-Jensen, Rev. Mod. Phys. 75, 607 (2003); and references therein.

[14] G.F. Bertsch and H. Esbensen, Ann. Phys. 209, 327 (1991).

[15] Y. Yu and A. Bulgac, Phys. Rev. Lett. 90, 161101 (2003).

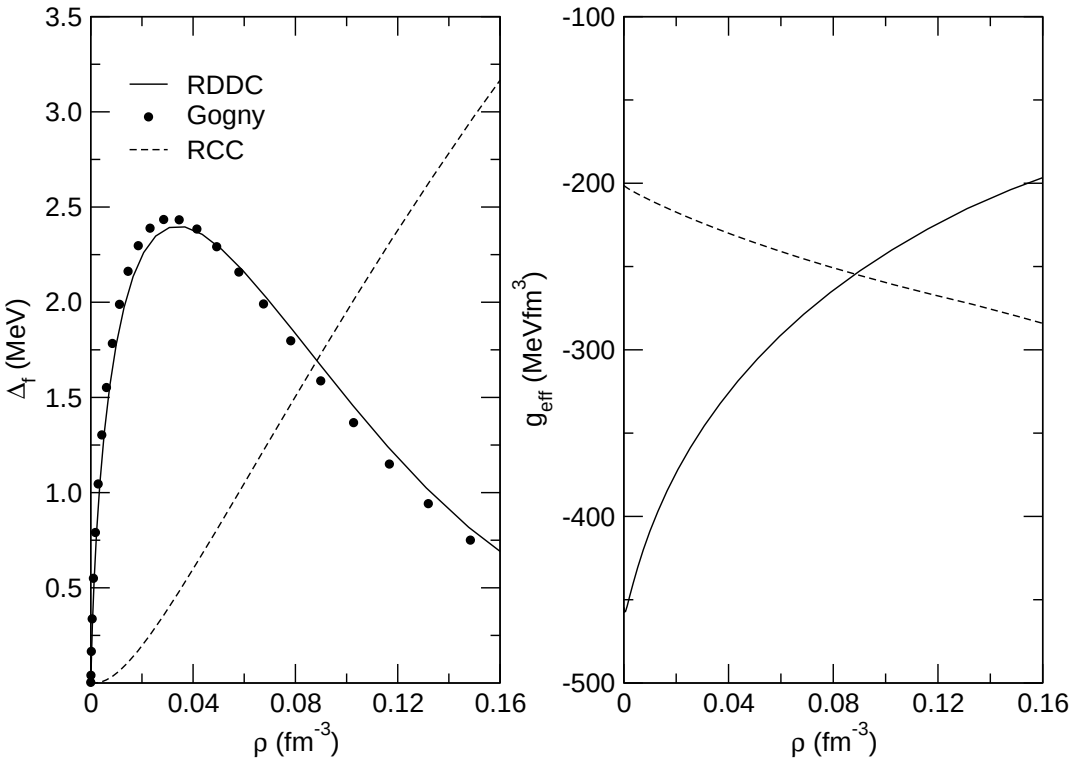


FIG. 1: Pairing gap in symmetric nuclear matter as a function of density for the zero-range interaction with constant coupling $g = -330$ MeV fm$^3$ (dashed) and the density-dependent coupling Eq. (23) (solid). The corresponding density-dependent curves $g_{\mathit{eff}}$ (Eq. (19)) are plotted in the panel on the right. The dots in the left panel denote the pairing gap calculated with the Gogny D1S interaction.

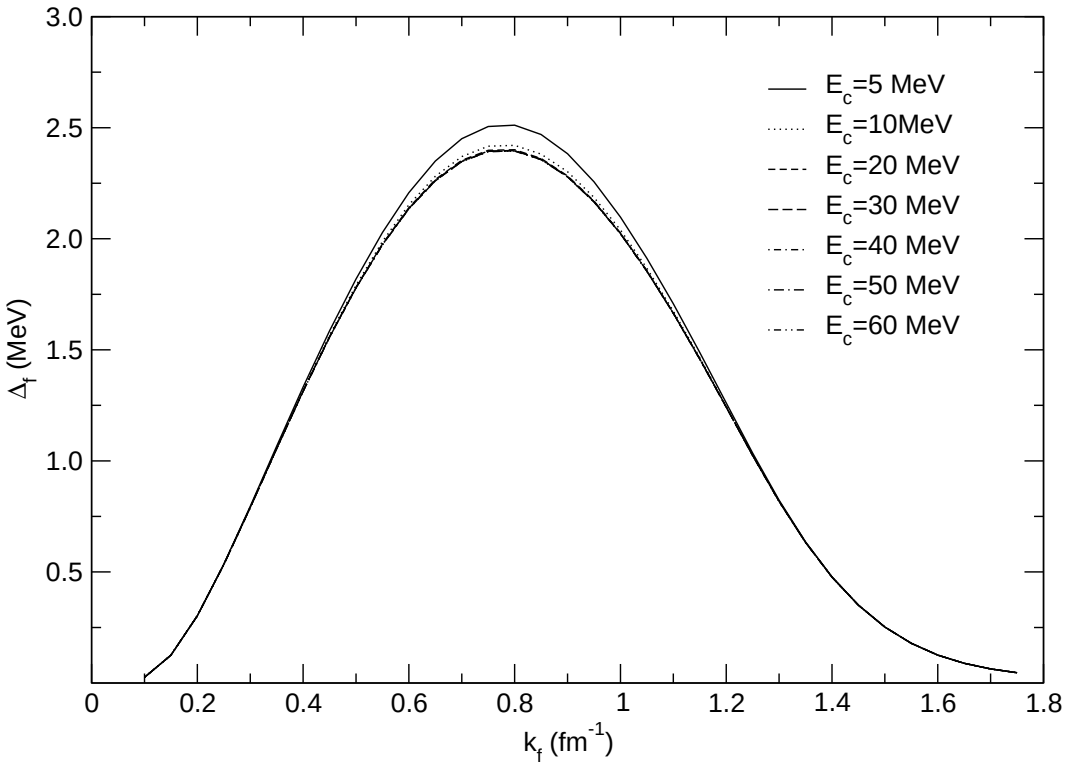


FIG. 2: Pairing gap in symmetric nuclear matter as a function of the Fermi momentum, calculated with the zero-range interaction and the density-dependent coupling Eq. (23), for a series of cut-off energies.

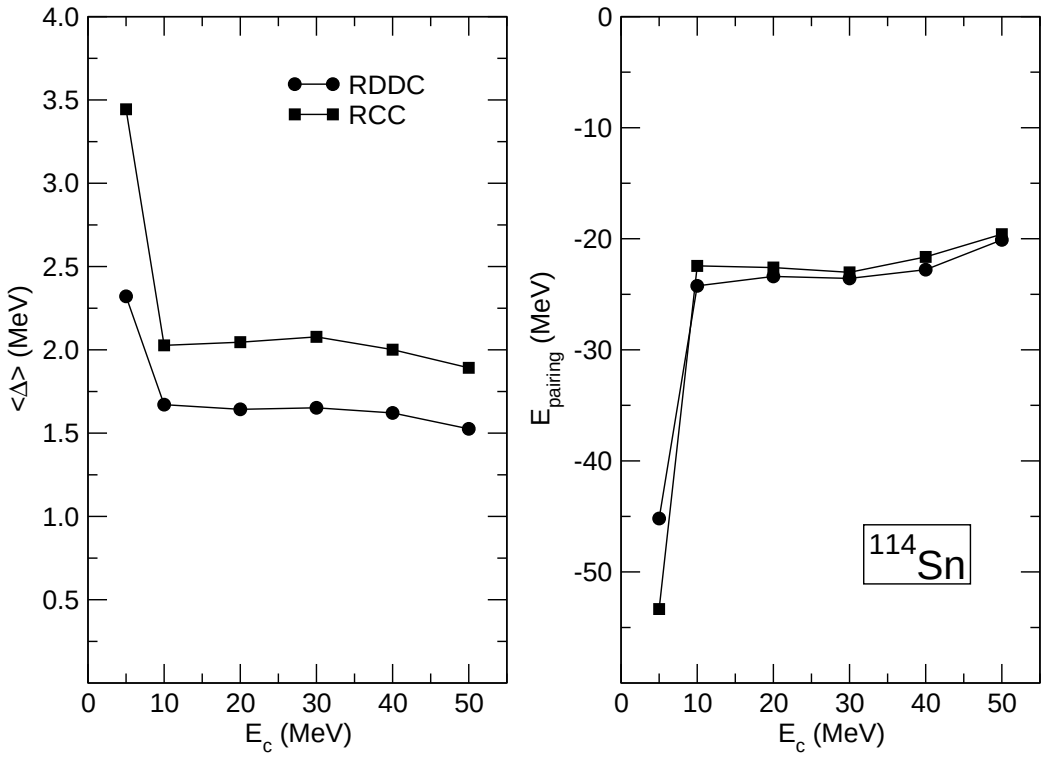


FIG. 3: Average neutron pairing gaps (left), and pairing energies (right) for $^{114}$Sn, calculated with a zero-range interaction, as functions of the cut-off energy. The calculations are performed with the renormalization of the constant coupling $g = -330$ MeV fm$^3$ (squares), and with the renormalization of the density-dependent coupling Eq. (23) (dots).

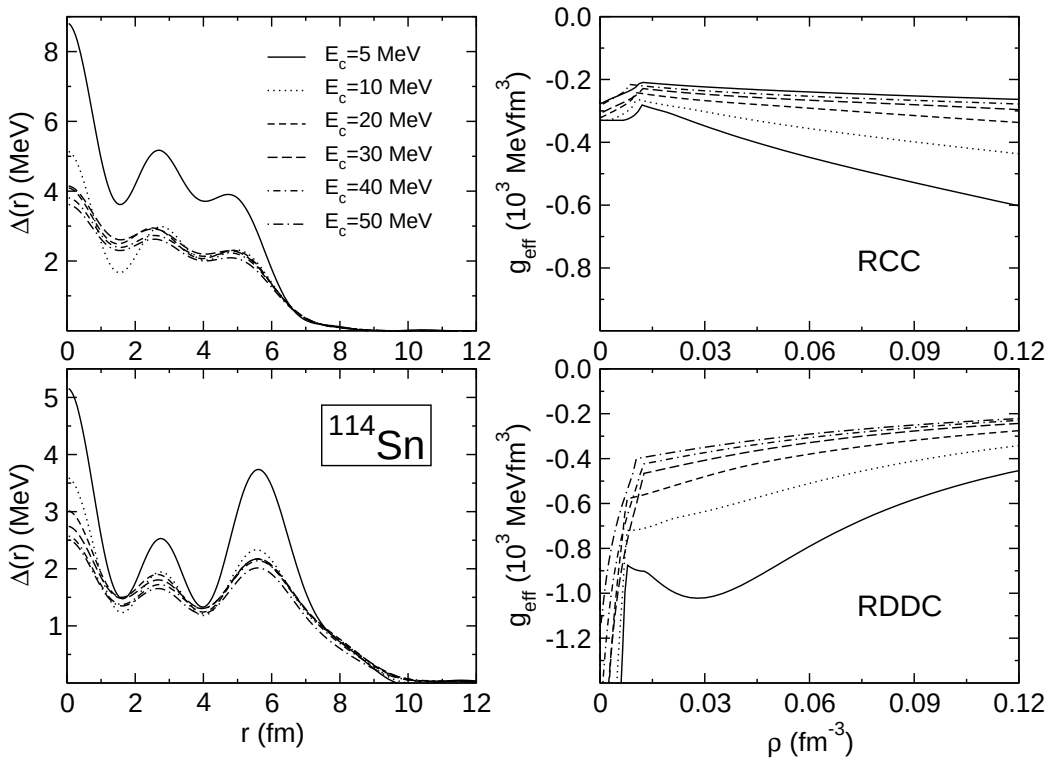


FIG. 4: The pairing fields as functions of the radial coordinate (left), and the curves $g_{\mathit{eff}}(r(\rho))$ (Eq. (19)) as functions of the corresponding density in $^{114}$Sn (right), for a series of energy cut-offs. The upper panels display results of the renormalization procedure for the zero-range force with constant coupling $g = -330$ MeV fm$^3$ (RCC), and the lower ones correspond to the density-dependent coupling Eq. (23) (RDDC).

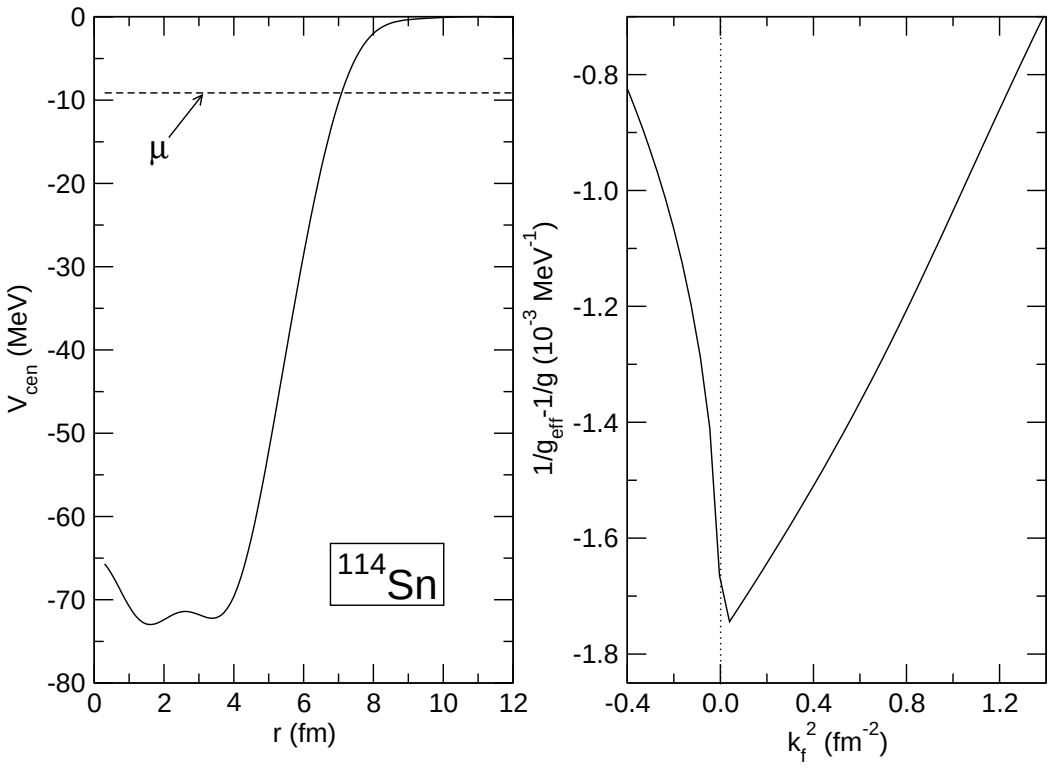


FIG. 5: The effective single-nucleon potential in $^{114}$Sn as a function of the radial coordinate (left), and the correction to the strength parameter of the zero-range effective force (right) as a function of the square of the Fermi momentum. $\mu$ denotes the position of the chemical potential.

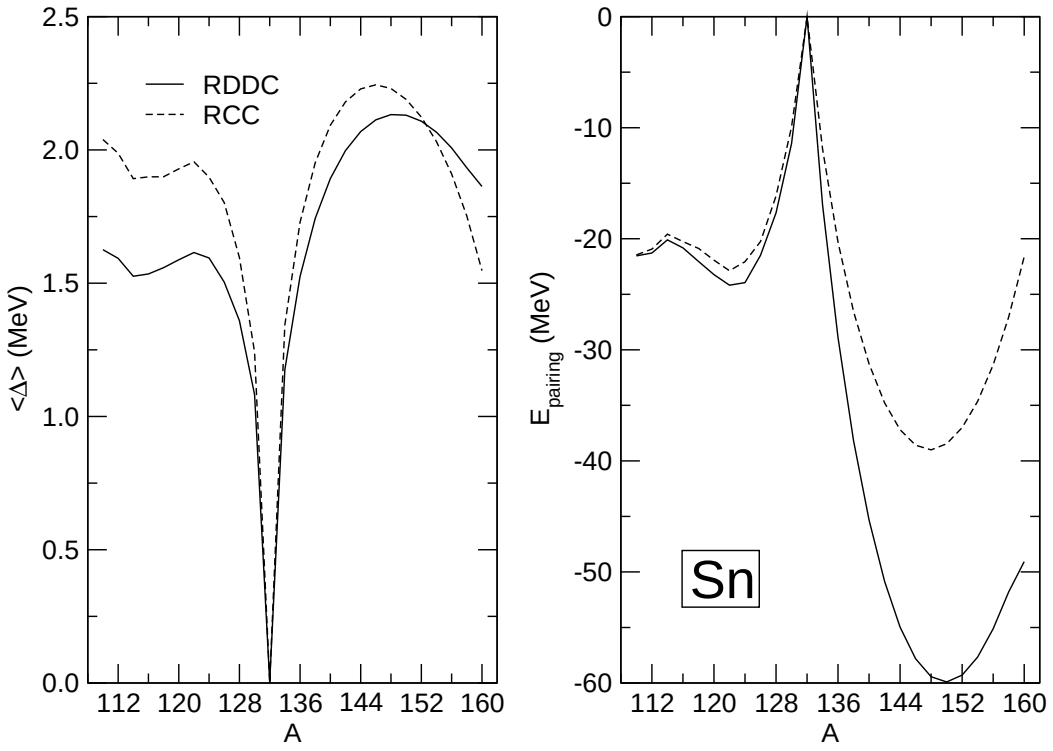


FIG. 6: Average neutron pairing gaps (left), and pairing energies (right) for the chain of even-even Sn isotopes with $110 \leq A \leq 160$. The calculations are performed with the renormalization of the constant coupling $g = -330$ MeV fm$^3$ (dashed), and with the renormalization of the density-dependent coupling Eq. (23) (solid).

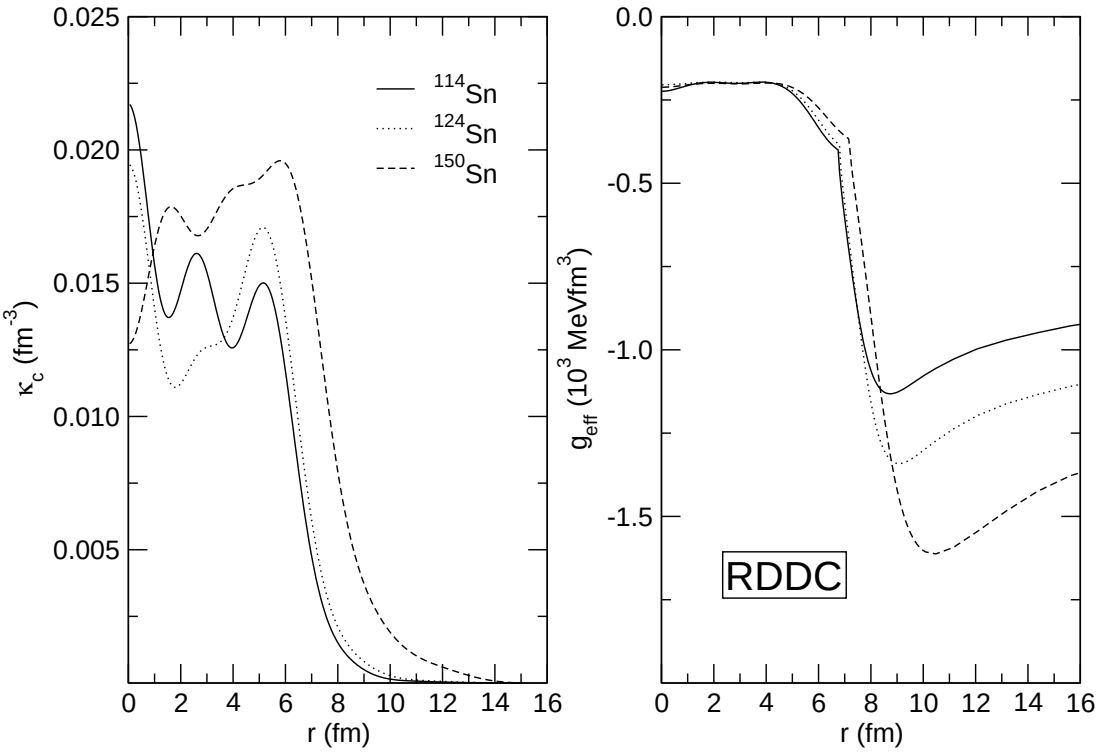


FIG. 7: The anomalous densities in $^{114}$Sn, $^{124}$Sn, $^{150}$Sn isotopes as functions of the radial coordinate (left), and the density-dependent curves $g_{eff}$ (Eq. (19)) (right). The calculations are performed with the renormalization of the density-dependent coupling Eq. (23) (RDDC).

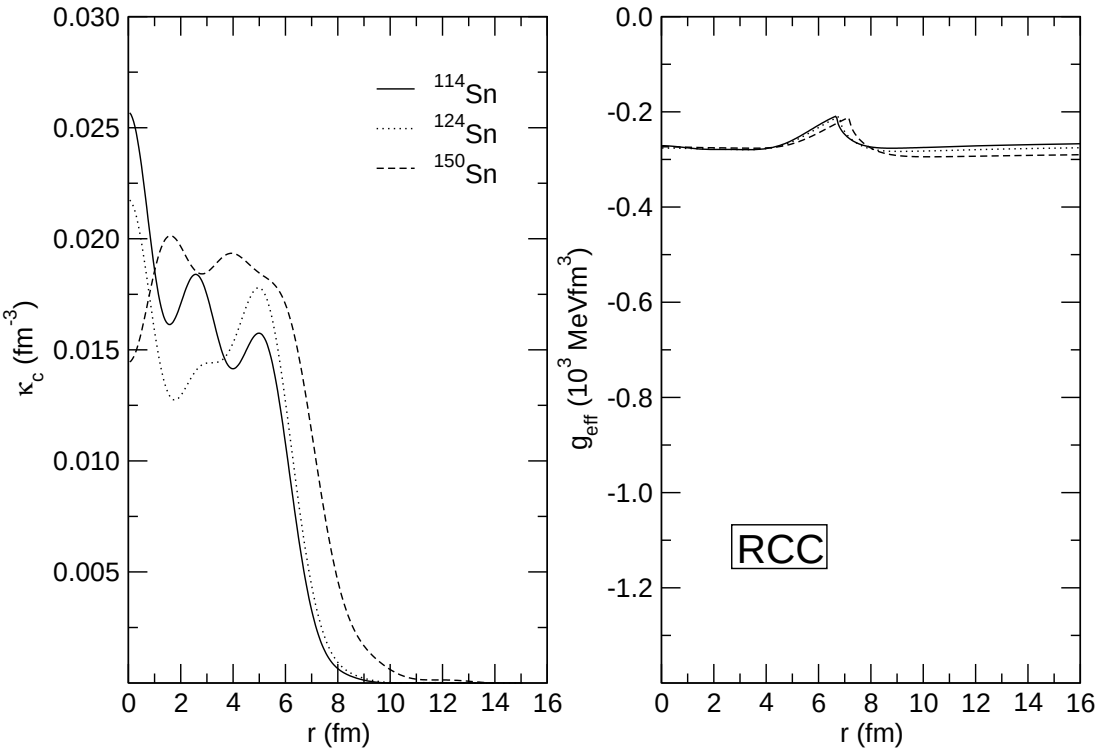


FIG. 8: Same as in Fig. 7, but for the RCC case with the constant coupling $g = -330$ MeV fm$^3$.